Time-Frequency Strain Data Analysis of Suspension Using the Hilbert-Huang Transform

Nadia Nurnajihah Mohamad Nasir [1]
Shahrum Abdullah[1,2]*
Salvinder Singh Karam Singh[1,2]
Mohd Faridz Yunoh[1]
Mohd Zaki Nuawi[1]
Sallehudin Mohd haris[1,2]
[1]Department of Mechanical and Materials Engineering,
Faculty of Engineering and Built Environment,
Universiti Kebangsaan Malaysia,
43600 Bangi, Selangor, Malaysia

[2]Centre for Automotive Research,
Faculty of Engineering and Built Environment,
Universiti Kebangsaan Malaysia,
43600 UKM Bangi, Selangor, Malaysia
**shahrum@ukm.edu.my*

ABSTRACT

This paper aims to study the application of the Hilbert-Huang transform in automotive component strain data. The objective is to analyse time-frequency strain data and investigate specific and indicative behaviour patterns of the time-frequency parameters by using the Hilbert-Huang transform. Hilbert-Huang transform is different from the traditional Fourier transform, which is used only for linear and stationary signals analysis. Fourier transform is different if compared with the Hilbert-Huang transform. Hilbert-Huang transform is designed to analysing the nonlinear and non-stationary signals and a more suitable tool for this kind of system. Empirical mode decomposition can characterise the intrinsic mode function to decompose the signal by mean of the time-frequency variations of signals. The empirical mode decomposition extracts both the original signals into a set of intrinsic mode functions which emphasises different oscillation mode with different amplitudes and frequencies. The intrinsic mode functions component produces significant and more effective physical analysis in the physical process at different time scales.

ISSN 1823- 5514, eISSN 2550-164X

Received for review: 2017-10-11
Accepted for publication: 2018-07-03
Published: 2018-11-30

The results obtained can also be observed from numerical parameters that there are difference between the wide inter-subject differences in the variance and the contribution period of each signal mode in intrinsic time-frequency to the total number of signal content. The mean period for both first decomposition signals is ~2 and ~6. Reconstruction of new signal is done using the result of decomposition signal, intrinsic mode functions and the residue. The reconstruction signals have a difference in the maximum amplitude less than 1.136×10^{-13} and 2.273×10^{-13} that indicate unknown noise. This study represents the decomposition signal which was at high frequency in the histogram of Kernel estimation probability based on the strain data signal in the automotive component.

Keywords: *Time-frequency analysis; Hilbert-Huang transform; life; strain data*

Introduction

Fatigue analysis is one of the analyses done on the automotive component to make sure the quality of component is in good condition. Material fatigue is among the most common safety issues which cause by cyclic loading and cause of failure. The existing methods in the time-frequency domain, widely used are Short-Time Fourier Transform (STFT), Wavelet Transform and S-Transform as mentioned by Yunoh [1]. The STFT had a fixed resolution and more applicable for real-time signal processing due to its short process time. While the Wavelet transform had good resolution and high performance in time and lower in frequency. It same with S-transform where it reduces the computational time. The signal represents a random phenomenon that depends on the time measurement. On account of the strain signal, the signal consists of an estimation of the cyclic loading such as stress and strain against time. The measurement of the signal regularly comprises of variation of frequency, amplitude, phase and energy. Djurović [2] stated that commonly the strain signal was found to exhibit a non-stationary behaviour.

Empirical mode decomposition (EMD) works to reduce a signal into a number collection of intrinsic mode functions (IMFs) with “well-behaved” Hilbert transform. It is proven to be versatile in extracting signals from data, including the nonlinear and non-stationary processes. EMD is widely applied in the mechanical fields, such as mechanical fault diagnosis by Lei [3] and Singh [4]. The substance of the method is to identify the characteristic intrinsic oscillatory modes by their trademark time scales in the data observationally and then decompose the data accordingly. Caesarendra et al. [5] were monitoring the natural damage on slewing bearing. They investigate the real data of bearing rotating speed and damages which are introduced the artificial fault. Each intrinsic mode is in a narrow condition and dominated by scales.

Thus, as indicated by the scale, the solid implications of every mode can be recognized. Not same as the Fourier transform where the representation permits a simultaneous understanding of the signal in both frequency and time in Yao [6]. However, Yang et al. [7] believe that, since the last IMF is constantly monotonic, fine-to-coarse neglects to separate the underlying pattern of numerous signals such as those signals whose hidden pattern are not monotonic. So, he suggested another pattern of extraction method based on the correlation of different IMFs. He changes the main data signal from time to frequency domain. Then, use the Hilbert-Huang transform and ascertain the marginal spectrums of each IMF. Finally, reconstruct of IMFs based on the correlation between various IMFs.

This study focuses on the time-frequency analysis technique, Hilbert-Huang transforms and one of the methods in this technique is EMD that uses strain data signal which contains nonlinear and non-stationary behaviour. This study proposes the use of EMD to analyse and investigate specific and indicative behaviour patterns of time-frequency parameters. Fourier transform is not suitable to analyse nonlinear and non-stationary signal because Fourier transform was in the nonlinear and stationary signal. The decomposition is generated by the number of IMF. IMF is used to reconstruct the original signal. It shows statistically significant in this method. On the IMF, histogram exists to show high frequency on each decomposition signals. In addition, the time-frequency analysis shows the shape of the probability density and cumulative density function based on the strain data signal of the suspension component in the automotive field.

Methodology

The methodology of this study is shown in Figure 1. The process flow starts by choosing the strain data signal. The signal is decomposed by the empirical mode decomposition which produces the specific independent component. The result of the decomposed signal and residue is used to recreate the new signal. The next step is to investigate the probability on Kernel distribution to observe the existence of a high-frequency condition in the decomposed signal. Lastly, each data signal was a plot in the reliability assessment by using two-parameter Weibull distribution to show the pattern of probability density function and cumulative density function.

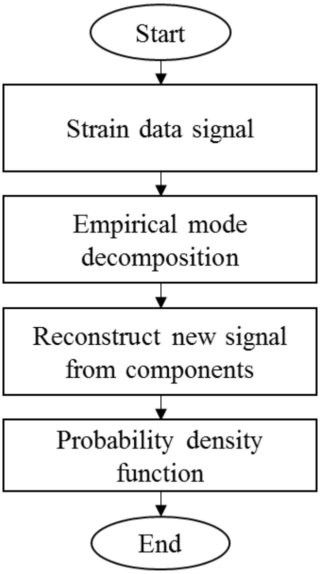

Figure 1 The flow process of the study

Type of signal

This study used two strain data signals from a suspension system which are made of carbon steel. One strain signal was from Society of Automotive Engineers (SAE), SAESUS. Another strain signal was measured from road test of resident road condition [8]. The material of SAE1045 was chosen because it is commonly employed in automotive industries to fabricate the coil spring [9]. In this study, both signals were addressed as S1 for SAESUS and S2 for resident road signal.

Hilbert-Huang Transform: Basic Empirical Mode Decomposition

The decomposition of the original data signal into few of finite IMFs by empirical mode decomposition (EMD). Then, intrinsic mode functions (IMFs) are reconstructed individually utilizing fine-to-coarse and correlation technique. The EMD method involves sifting an ensemble of noise-added signal and made the mean as the final result. Like EMD, original data $x(t)$ can also be represented as

$$x(t) = \sum c_i(t) + r_n \tag{1}$$

The residue r_n appeared and the complete sifting process will stop, it becomes as a monotonic which the will no IMF can be extracted, and the detail can be found in Huang et al. [10]. There are two conditions which satisfy the function of the IMF definition. They are [11]:

- The number of extrema and therefore the number of zero-crossings in the entire data series must be equivalent or vary at the most by one.
- At any instance in time, the mean value of the envelope described by the local maxima and minima is zero.

Reconstruction Signal from Each Component

Fine-to-coarse is a reconstructed technique which depends on the alter of the data structure from the original. The procedures follow [12]:

- Calculate the mean of the total of $c_1(t)$ to $c_i(t)$ for every segment (aside from the residue);
- Use a t-test to recognize when *i*, the mean, significantly different from zero;
- Once i is recognized as a huge change point, incomplete reconstruction with IMFs from this to the end is distinguished as the low-frequency mode while fractional reconstruction with different IMFs, recognized as a high-frequency mode.
- The residue is specifically viewed trends of original data.

The probability of Data Signal

Histogram

Histograms are one of density estimation methods that are used widely. The data range is divided into one set of successive intervals and not overlap called bins. The histogram bins are defined as the intervals,

$$x_0 + mh, x_0 + (m+1)h \tag{2}$$

for m positive and negative integers, x_0 is the origin and h is the bin width. For a set of n, observed data points are supposed to be samples of an unknown density function p_x. The histogram is defined by

$$\hat{p}_x(x) = \frac{\text{number of observations in the same bin as } x}{nh} \tag{3}$$

The histogram can be generalised by allowing the bin widths to vary. Then the formula becomes

$$\hat{p}_x(x) = \frac{\text{number of observations in the same bin as } x}{n \text{ (width of bin containing } x)} \tag{4}$$

The Kernel Estimator

The density of the kernel estimator is obtained by replacing the weight function in the expression of the naive estimators by kernel function $K(x)$ which satisfies

$$\int_{-\infty}^{+\infty} K(x)\,dx = 1 \tag{5}$$

Then, the kernel estimator is given by

$$\hat{p}_x(x) = \frac{1}{nh}\sum_{i=1}^{n} K\left(\frac{x-x_i}{h}\right) \tag{6}$$

Here h is the smoothing parameter. It controls the trade-off between the statistical significance of the probability density function (PDF) estimation and it is an effective resolution.

Weibull Distribution

By performing a simple linear regression, parameters α, the featured life we can be obtained, which is a scale, or spread, in data distribution and β, the shape parameter that indicates whether the failure rate is increasing. When a linear regression is performed, the estimation for the Weibull β parameter comes directly from the slope of the line. The estimation for the α parameter should be calculated as:

$$\alpha = e^{-\left(\frac{b}{\beta}\right)} \tag{7}$$

The probability density function (PDF) and cumulative distribution function (CDF) for two-parameter Weibull distribution are provided as

PDF: $$f(x) = \frac{\beta (x)^{\beta-1}}{\alpha^{\beta}} \exp\left[-\left(\frac{x}{\alpha}\right)^{\beta}\right] \tag{8}$$

CDF: $$F(x) = 1 - \exp\left[-\left(\frac{x}{\alpha}\right)^{\beta}\right] \tag{9}$$

Mean-time-to-failure (MTTF), two-parameter Weibull distribution is calculated from the MTTF equations

$$MTTF = \alpha\Gamma\left(\frac{1+\beta}{\beta}\right) \tag{10}$$

where (г) is gamma function.

Result and Discussion

To represent the kind of results obtained from empirical mode decomposition (EMD) in Figure 2 and Figure 3, the intrinsic mode function (IMF) components obtained from the two signals are shown. Both signals decomposition yields 10 components and a residue. Each IMF has a particular amplitude and frequency content.

The signals variation is due to the nature information of the IMFs. An exceptional advantage of the decomposition is that it is probable to observe directly the local variation in the strain data signal. The intrinsic oscillations appear naturally and based on the experience of the monitored or observed phenomena, the conclusions can be obtained the meaning from each mode and associated to some behaviours. In Figure 2 and Figure 3 there are residues that keep the mean without fast and short lasting oscillations. The trend is nonlinear, a hallmark of the non-stationary process is in negative as it declines over time scales.

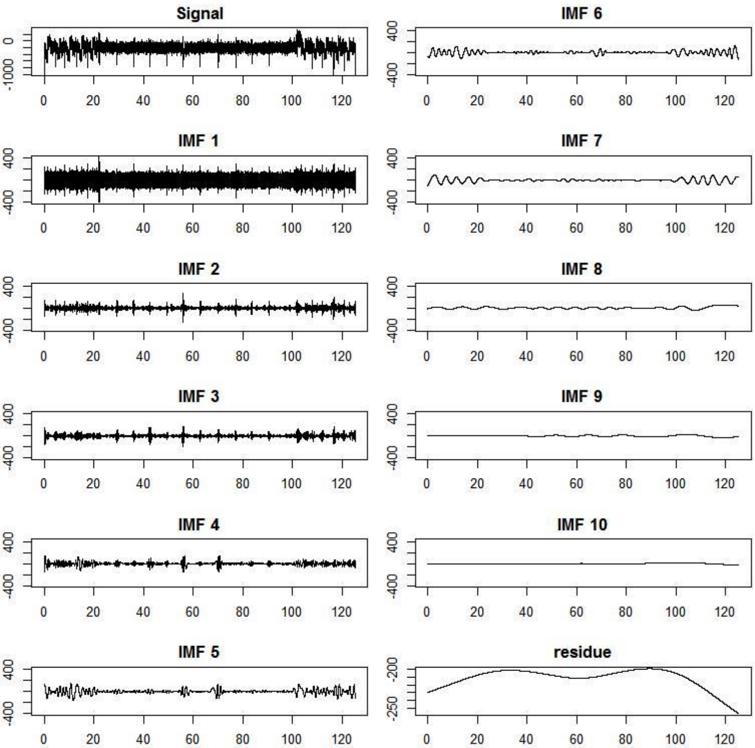

Figure 2 Decomposition of S1 signal

One of the necessary conditions for the basis to representing time series is nonlinear and non-stationary time is completeness, which ensures the level of accuracy of the expansion. Once the signals have been decomposed into IMFs, the criteria are marked numerically. Theoretically, completeness has been proven by Huang et.al [10].

The restructuring of the selected signal as an example is shown in Figure 4. The original data is represented in the dashed line and the components are rebuilt in the solid line (red). By adding residue to each component, starting from the longest component to the most limited, IMF 1 in Figure 4 (k), the original signal is reproduced. When the reconstruction reaches IMF 3 and IMF 2 in Figure 4 (i-j), the original series can be restored practically and the amount energy is contained in the original strain data signal. The new component, IMF 1 does not significantly contribute to reassemble the signals.

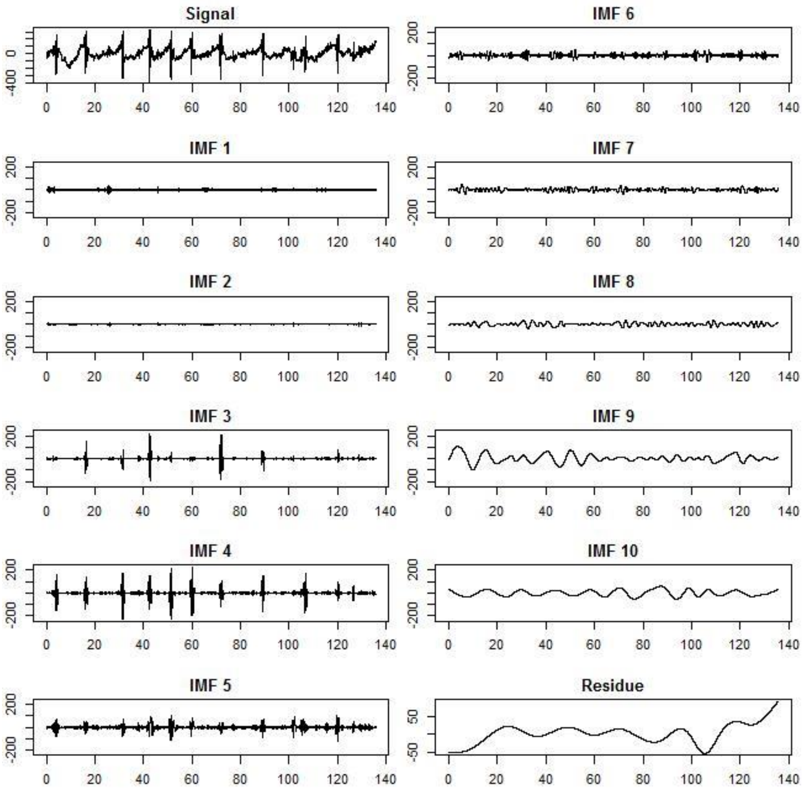

Figure 3 Decomposition for S2 road signal

Completeness is numerically checked for the whole strain data set. The difference between the reconstruction data obtained from the sum of all the IMFs and original data for the S1 road are shown in Figure 4 (l) where the maximum amplitude is less than 1.136×10-13 for the resident signal. For S1 signal the maximum amplitude is less than 2.273×10-13 in Figure 5. This difference is due to the unknown noise existing in the first original signal [13]. Thus, the signal represents completeness that is established numerically in Figure 4.

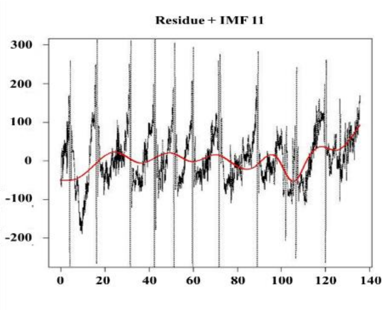
Residue + IMF 11
300
200
100
0
-100
-200
0
20
40
60
80
100
120
140

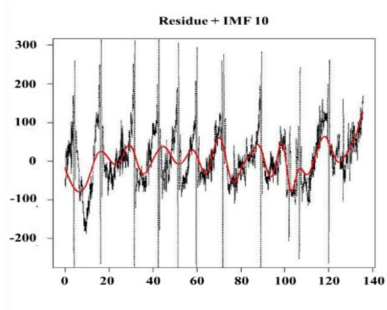
Residue + IMF 10
300
200
100
0
-100
-200
0
20
40
60
80
100
120
140

(a)

(b)

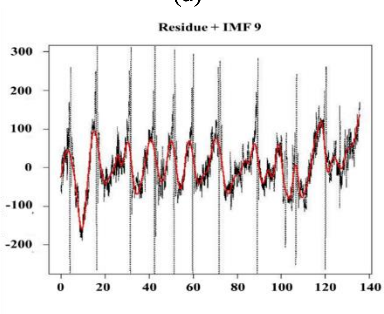
Residue + IMF 9
300
200
100
0
-100
-200
0
20
40
60
80
100
120
140

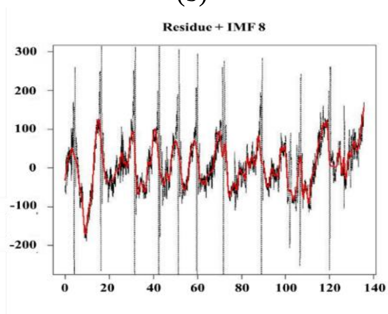
Residue + IMF 8
300
200
100
0
-100
-200
0
20
40
60
80
100
120
140

(c)

(d)

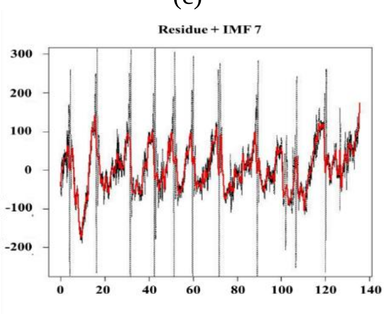
Residue + IMF 7
300
200
100
0
-100
-200
0
20
40
60
80
100
120
140

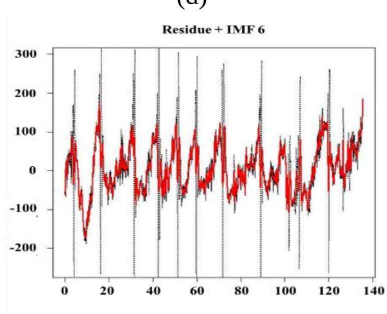
Residue + IMF 6
300
200
100
0
-100
-200
0
20
40
60
80
100
120
140

(e)

(f)

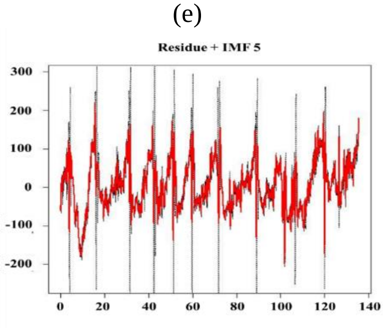
Residue + IMF 5
300
200
100
0
-100
-200
0
20
40
60
80
100
120
140

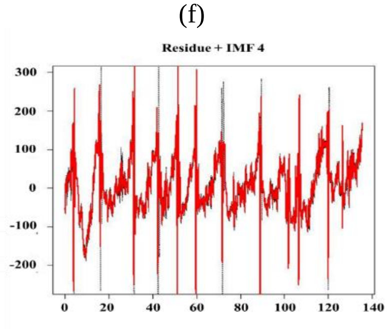
Residue + IMF 4
300
200
100
0
-100
-200
0
20
40
60
80
100
120
140

(g) (h)

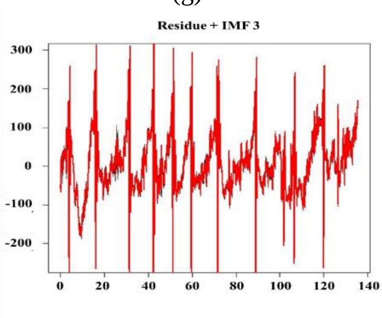

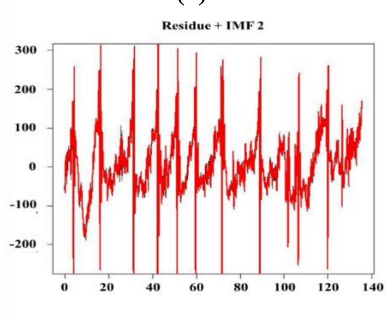

(i) (j)

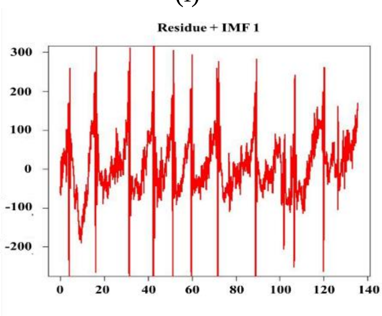

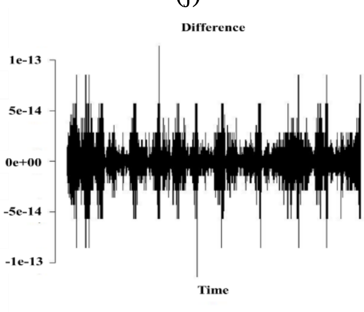

(k) (l)

Figure 4 Reconstruction of S2 signal

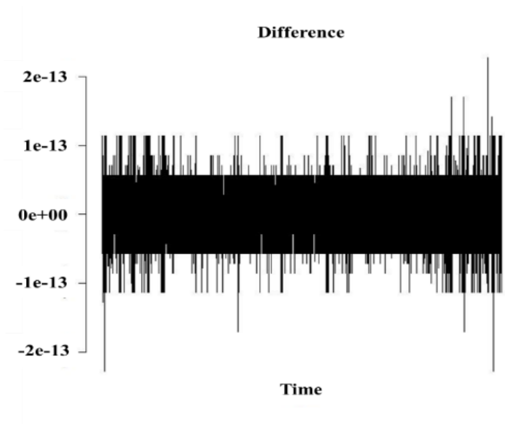

Figure 5 Difference of reconstruction for S1 signal

IMF Statistics

The IMF component was existing was showing the frequency of each decomposition signals can change without affecting the time. The duration of the signal is inconsistent. The IMF period can be calculated by dividing the number of data points with the number of peaks or maxima. Therefore, if T is the length of the IMF component and s is the peak number, then the IMF period is equal to T/s.

A graph in Figure 6 shows the difference mean period of IMFs between S1 and S2. The period is more noteworthy as the mode number is higher. After modification of the numerical result, in the entire data set collection, it is presumed that the EMD is a dyadic filter, which is a mean

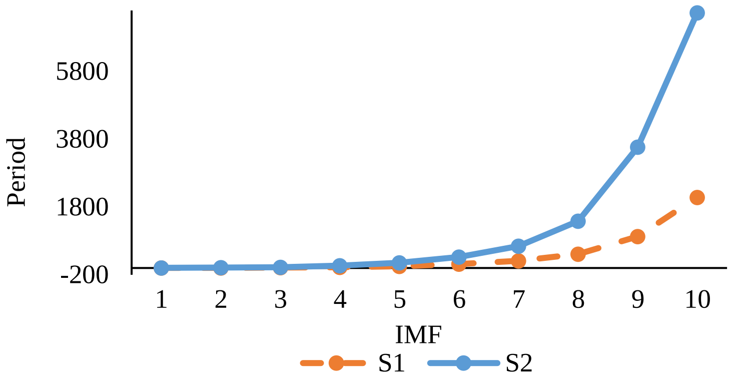

Figure 6 The mean period between S1 and S2 signal

period of IMFs component for both roads was exactly increased starting from IMF 5 to IMF 10. The first mode of IMF has the smallest mean (~2 and ~6) and for progressive components, the mean period doubles. For the latest IMF mode, the instability of the period is evident from incentives that are close to zero to the maximum value reaching thousands, which are characteristic of moderate motion of oscillations.

The mean duration was calculated, and the value is listed in Table 1. Each decomposition signal represents a specific behaviour found in both data signals. The segments demonstrate the data signals while every column is the content of the run of time in each decomposed mode. Regarding the doubling period, it is more obvious in the first mode and can not clearly verify for the last two modes, which is due to the increasingly close component of the noisy when the decomposition procedure approaches the residue.

Observation in Figure 6, show that there is no significant period contrasts in the entire data signal while each mode been analysed independently and it notices that the period essentially changes in eighth IMF.

Table 1 Contribution of the period from the decomposition signal.

IMF	S1	S2
1	2.368	6.071
2	4.129	10.430
3	9.344	26.008
4	22.619	66.239
5	55.324	158.850
6	112.891	324.540
7	208.850	645.990
8	410.852	1384.265
9	928.222	3569.947
10	2088.500	7536.555

The average contribution of variance from each IMF is also calculated. These variances are used as a basic and intuitive benchmark to determine the importance of each IMFs of the original signal. The component with greater variance is more important.

Table 2 Variance value of signal

IMF	SAESUS			Resident		
	Var	**Var (%)**	**∑ (%)**	**Var**	**Var (%)**	**∑ (%)**
1	10409.600	56.025	56.025	8.209	0.189	0.189
2	1143.383	6.154	62.179	1.149	0.026	0.215
3	1064.201	5.728	67.907	406.965	9.367	9.583
4	1096.906	5.904	73.810	1037.362	23.878	33.461
5	1893.335	10.190	84.000	441.611	10.165	43.625
6	1218.010	6.555	90.556	224.795	5.174	48.800
7	1056.199	5.685	96.240	151.360	3.484	52.284
8	442.184	2.380	98.620	183.767	4.230	56.514
9	180.364	0.971	99.591	1224.314	28.181	84.695
10	76.022	0.409	100.000	664.943	15.305	100.000

The contribution of each IMFs to the total variance also changes from signal to signal. Table 2 lists the contribution of each IMF to the total sum of variance for a selected subject in absolute terms, the percentage of total variance and the cumulative percentage variance contribution. The variance is calculated by the sum of, $\frac{(X-\mu)^2}{N}$, where μ mean, N the total number of data and X is the data value. Using the variance value, it is possible to see the significant differences in the contribution of the variance of each IMF to the amount of variance in the selected signals.

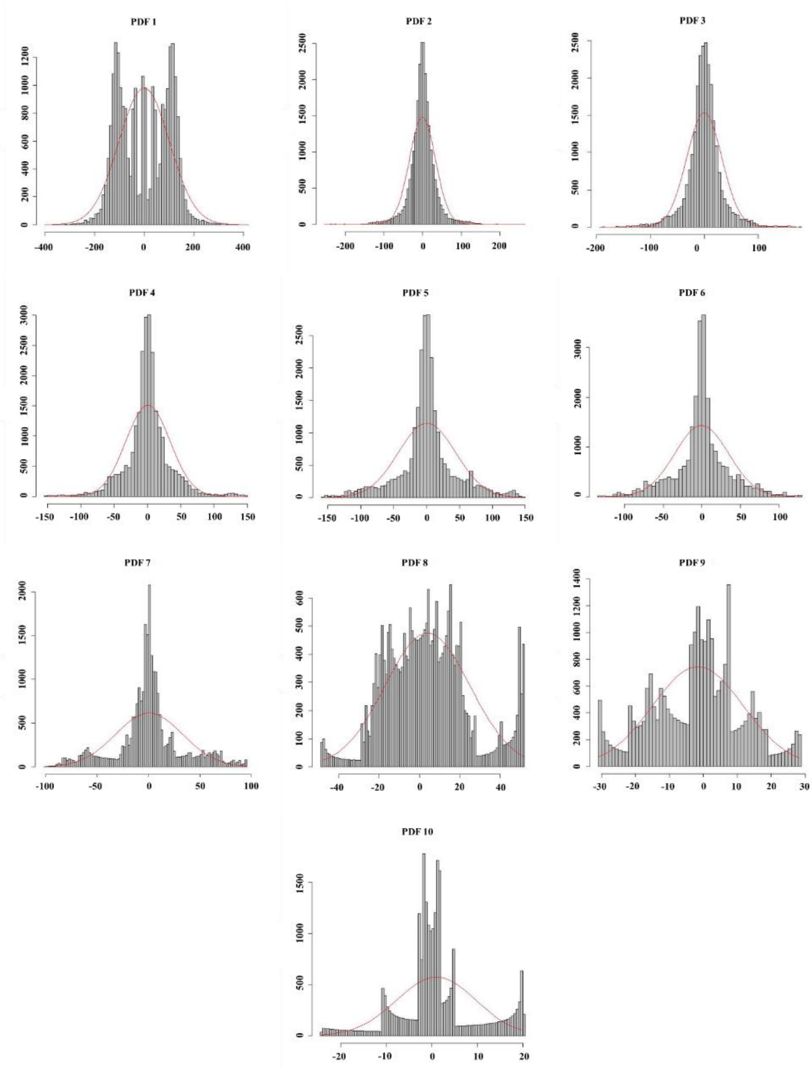

(a) Probability function density of S1

The probability distribution of the individual IMF calculated for both data signals is shown in Figure 7. According to the Central Limit Theorem, when the sample size is large, the IMF of high-frequency modes will have more oscillations and therefore the probability density function (PDF) will follow the normal distribution. This is shown from the normal distribution function installed with a red line. It is observed that the mean of these distribution functions is about zero in the whole set of data. The difference between the inter mode and intersubject is based on the deviation size of the normal distribution function. It is not a wide and narrow tendency to deviation from the normal distribution function when the number of modes increases. The deviation increases when the modes index increase in Figure 7 (a) and Figure 7 (b) the increasing tendency that occurs in high-frequency modes. These will coincide with the previous results where it is noted that for phenomenon analysed in population, it is possible to select certain components of IMF as having the highest energy content. The probability density function energy for the normal distribution series should have x^2 distribution.

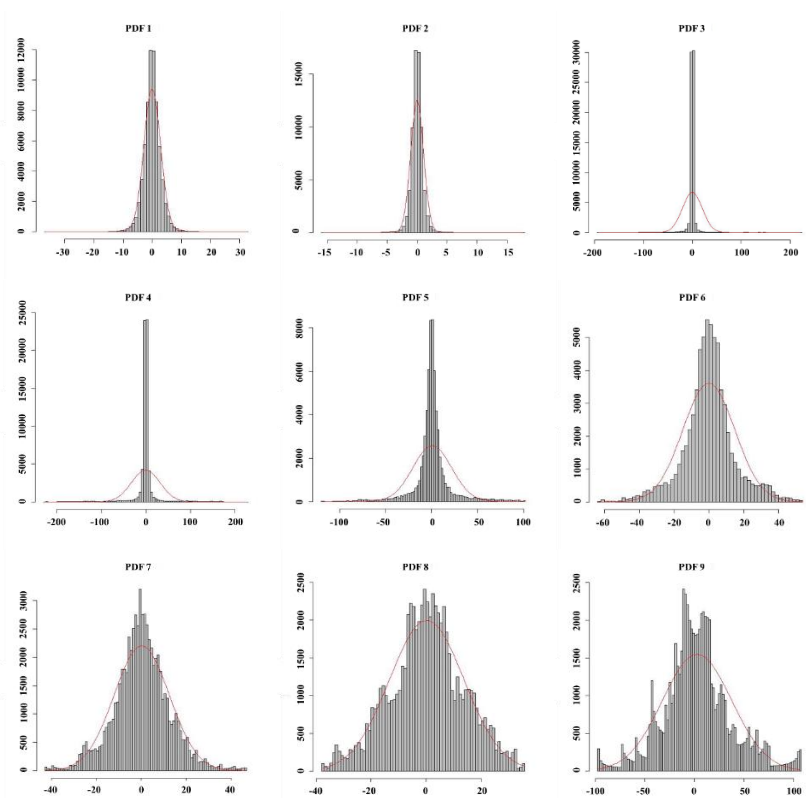

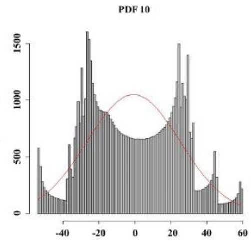

(b) Probability function density of resident road

Figure 7 Probability function density of each IMF signal using the Kernel's distribution for (a) S1 and (b) S2 signal.

The Weibull Distribution Analysis

The Weibull distribution was known as the distribution of extreme values to control the load as a measurement of the period in the failure process. Probability density function (PDF) and cumulative distribution function (CDF), as shown in Figure 8 and Figure 9, characterisation of Weibull distribution based on the approximate form of the shape (β) and obtained in the normal probability graph [14]. They show the prediction of critical parameters that contribute to the fatigue life in each IMF. The shape parameter (β) is evaluated to be greater than 1 indicates that failure occurs was expected to the deteriorating of the damage for each IMF signal.

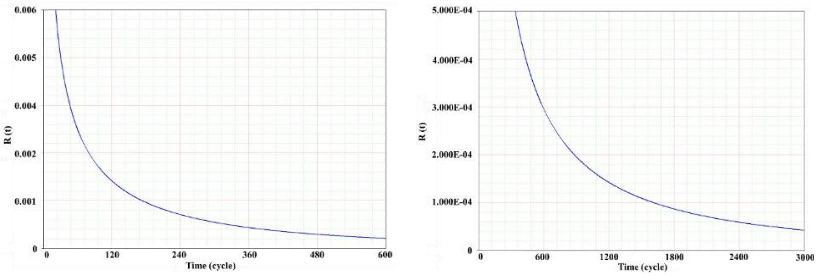

(a) (b)

Figure 8 The PDF Weibull of the number of cycles, (a) S1 and (b) S2

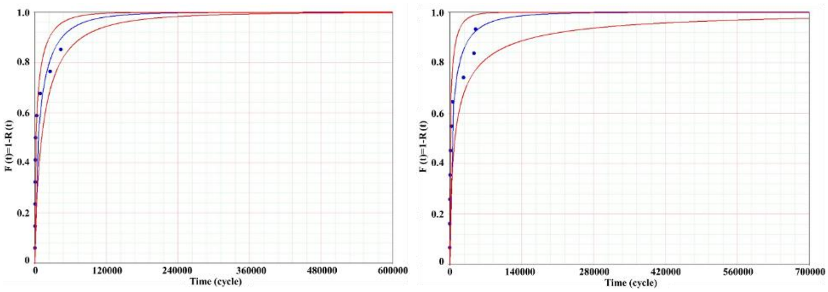

(a) (b)

Figure 9 The CDF Weibull of the number of cycles, (a) S1 and (b) S2

The graph shows in Figure 9, the cycle value in the safe range but there are two data for S1 and one data for S2 which are out of the distribution range. At that point, they are considered as being in failed condition. The mean load to failure was figured from the estimation of the shape parameter (β). The shape parameter (β) for S1 is 0.5645 and 0.4825 for S2 was estimated based on the Weibull distribution characterisation in Table 3. Based on the characteristic of the shape parameter, $0 < \beta < 1$, it indicates an increasing failure rate because this shape parameter is run to failure policy [15]. Mean-time-to-failure values are 282.589 cycle and 1487.922 cycles for S1 and S2. Mean-time-to-failure is the average time when the item will work before it fails. It is the mean lifetime of the item. With the data strain signals, the arithmetic average of the data does not provide a good measure of the centre because at least some of the failure times are unknown.

Table 3. Theoretical properties of shape parameter, β

Shape parameter, β	**Properties**
$\beta < 1$	Decreasing failure rate
$\beta = 1$	Constant failure rate
$\beta > 1$	Increasing failure rate

Conclusion

Empirical mode decomposition (EMD) method is widely used in engineering because it is intuitive, direct and adaptive. In implementing the EMD, it is imperative to build the IMFs to facilitate analysis and provide a diverse array of time scales data. The main reconstruction method is to see the difference of the decomposition signal to recreate original data. The difference of the maximum amplitude after reconstruction is less than 2.273×10^{-13} and 1.136×10^{-13} for both signals. EMD was implemented to decompose the original strain data signal by obtaining the IMF mode to demonstrate the non-stationary behaviour. The EMD analysis breaks the signal into a set of natural oscillations (IMFs) that have significant statistics to see the difference in duration and the contribution of the variance from each mode to the number of signals.

Besides that, the fatigue life cycle of the decomposed signal (IMFs) for both signals is seen through the Weibull distribution. The PDF and CDF for both signals were estimated the shape parameter for S1, 0.5645 and S2, 0.4825 where the value between zero and one indicates a rising rate of failure. The mean-time-to-failure value of S1 and S2 are 282.589 cycle and 1487.922 cycles respectively. From the data distribution, it shows the hidden information that the strain data signal is going to fail. This study was investigating the strain data signal behaviour with the decomposition method of Hilbert-Huang transform, empirical mode decomposition which can appear while it was hidden in the original signal.

Acknowledgements

The authors acknowledge the financial support from the Universiti Kebangsaan Malaysia (UKM) and the Ministry of Education, Malaysia through a research sponsorship with Grant No. FRGS/1/2015/TK03/UKM/01/2.

References

[1] M. Yunoh, S. Abdullah, M. Z. Nuawi, and Z. M. Nopiah, “ A review of localised time-frequency features classification associated to fatigue data analysis,” International Review of Mechanical Engineering 7(5), 960-976 (2013).

[2] I. Djurović, L. Stankovic, M. Rupp, and L. Shao, “Robust processing of nonstationary signals,” Journal on Advances in Signal Processing, vol 2010. Springer (2010).

[3] R. Jiang, and D. Murthy, “A study of Weibull shape parameter: properties and significance,” Reliability Engineering & System Safety 96(12), 1619-1626 (2011).

[4] S. Singh, and N. Kumar, "Combined rotor fault diagnosis in rotating machinery using empirical mode decomposition,” Journal Mechanical Science and Technology 28(12), 4869-4876 (2014).

[5] W. Caesandra, P. B. Kosasih, A. K. Tieu, S. A. S. Moodie, and B. -K. Choi, “Condition monitoring of naturally damaged slow speed slewing bearing based on esemble empirical mode decomposition,” Journal of Mechanical Science and Technology 27 (8), 2253-2262 (2013).

[6] X. Yao, X. Sun, Y. Yang, D. Wu, and X. Liang, "Features Extraction and Reconstruction of Country Risk based on Empirical EMD," Procedia Computer Science 31, 265-272 (2014).

[7] Z. Yang, B. W. -K. Ling, and C. Bingham, "Trend extraction based on separations of consecutive empirical mode decomposition components in Hilbert marginal spectrum," Measurement 46(8), 2481-2491 (2013).

[8] M. F. M. Yunoh, S. Abdullah, M. Z. Nuawi, and Z. M. Nopiah, "Durability analysis of motorcycle frame using fatigue I-kaz technique," Applied Mechanics and Materials. Trans Tech Pulb (2014).

[9] Y. Prawoto, M. Ikeda, S. K. Manville, and A. Nishikawa, A. "Design and failure mode of automotive suspension springs," Engineering failure analysis 15(8), 1155-1174 (2008).

[10] N. E. Huang, Z. Shen, S. R. Long, M. C. Wu, H. H. Shih, Q. Zheng, N. -C. Yen, C. C. Tung, and H. H. Liu, "The empirical mode decomposition and the Hilbert spectrum for nonlinear and non-stationary time series analysis," Proceedings of the Royal Society of London A: Mathematical, Physical and Engineering Sciences. The Royal Society (1998).

[11] G. Rilling, P. Flandrin, P. and P. Goncalves, "On empirical decomposition and its algorithms," IEEE-EURASIP workshop on nonlinear signal and image processing. IEEER (2003).

[12] X. Zhang, K. K. Lai, and S. -Y. Wang, "A new approach for crude oil price analysis based on empirical mode decomposition. Energy economics 30(3), 905-918 (2008).

[13] Y. Pei, Y. Wu, and D. Jia, "Research on PD signals denoising based on EMD method," Journal of Electronic 88, 137-140 (2012).

[14] H. Li, D. Wen, Z. Lu, Y. Wang, and F. Deng, "Identifying the Probability Distribution of Fatigue Life Using the Maximum Entropy Principle," Entropy4 (18), 111 (2016).

[15] R. Jiang, and D. Murthy, "A study of Weibull shape parameter: properties and significance," Reliability Engineering & System Safety 96(12), 1619-1626 (2011).